https://doi.org/10.1142/9789811278952_0015

Chapter 15

Energy Deposition and Radiation to Electronics

F. Cerutti[a], R. Garcia Alia[a] and A. Tsinganis[b]

[a]*CERN, SY Department, Genève 23, CH-1211, Switzerland*
[b]*CERN, EP Department, Genève 23, CH-1211, Switzerland*

The radiation impact on the machine elements and the electronics equipment in the high luminosity insertions is discussed, distinguishing the different loss regions, and respective mitigation measures are highlighted.

1. Collision Debris

Proton–proton inelastic collisions* taking place in the LHC inside its four big detectors generate a large number of secondary particles, mostly pions. The average multiplicity for one collision at 7 TeV beam energy is about 120 [1-4], but there are very substantial fluctuations over different events. Moving from the interaction point (IP), this multiform population evolves, even before touching the surrounding material, because of the decay of unstable particles, in particular neutral pions decaying into photon pairs. Most of these particles are intercepted by the detector and release their energy within the experimental cavern. However, the most energetic ones, emitted at small angles with respect to the beam direction, travel farther in the vacuum tube and reach the accelerator elements beyond the TAS (Target Absorber Secondaries) absorber, a protection element consisting of a 1.8 m long copper core located

* From the perspective of the radiation impact in the experimental insertions, ion–ion collisions remain in the shadow of the proton operation, because of their much lower luminosity, except for some remarkable processes, such as the Bound Free Pair Production, originating very localized losses with major implications on the LHC upgrade strategy, as discussed in Chapter 8.

at 20 m from the IP and featuring in the HL era a circular aperture of 60 mm diameter. Despite the fact that on average the number of particles per collision leaving the TAS aperture is more than one order of magnitude lower than the total number of debris particles, they carry about 80% of the total energy, 40% for each side. At the nominal HL-LHC luminosity (5×10^{34} cm^{-2} s^{-1}), this represents about 3800 W per side that is impacting the LHC elements and is dissipated in the machine, in the nearby equipment and in the tunnel walls.

2. Triplet and Separation Dipole Protection

The TAS absorber is part of the interface area between the detector and the accelerator on each side of the high-luminosity IRs, namely IR1 and IR5, hosting the ATLAS and CMS detectors respectively (see Figure 1, left panel). Its protection role is not needed for luminosities up to 0.2×10^{34} cm^{-2} s^{-1}, as in the LHCb insertion [5], and is in fact limited to the first quadrupole, since its geometrical shadow gets quickly dashed by the effect of the magnetic field that bends a significant fraction of charged debris particles coming through the TAS aperture, in particular high energy pions, against the quite larger quadrupole aperture.

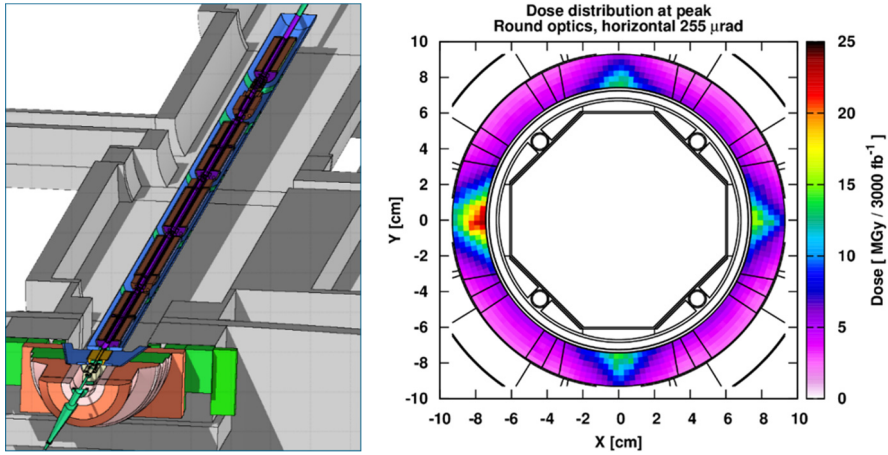

Fig. 1. Left: Geometry model [6,7] of the future machine layout outside the CMS cavern. In the forefront at the bottom, the TAS is surrounded by the visible massive shielding. Right: Dose distribution in the quadrupole coils at the most exposed location. The mid-planes hot spots are mitigated by tungsten alloy absorbers attached to the octagonal beam screen.

For this reason, the backbone element for the protection of the string of magnets up to the separation dipole (D1) will instead be the beam screen equipped with dedicated tungsten alloy absorbers all over its length, reaching their maximum thickness (of 16 mm in the first quadrupole and 6 mm elsewhere) at the magnet mid-planes, where the energy deposition is concentrated, as shown in the right panel of Figure 1.

The combination between the focusing-defocusing field configuration and the crossing plane yields a characteristic longitudinal profile for the peak dose (or power density) in the superconducting coils, as reported in Figure 2. After the HL-LHC upgrade, the weakest point becomes the IP end of the third quadrupole (Q2b) for horizontal crossing, due to the effect of the preceding interconnect, where the amount of absorbing material is limited. A careful optimization of the interconnect design, allowing for the extension of the tungsten alloy absorbers as well as their installation in the embedded Beam Position Monitor (BPM), brought the maximum dose expectation below 30 MGy for the nominal target of 3000 fb^{-1}, which is a level deemed to be still sustainable by the coil insulator. On the other hand, the maximum power density is predicted not to reach 3 mW/cm^3 at 5×10^{34} cm^{-2} s^{-1}, so remaining safely below the quench limit [8,9].

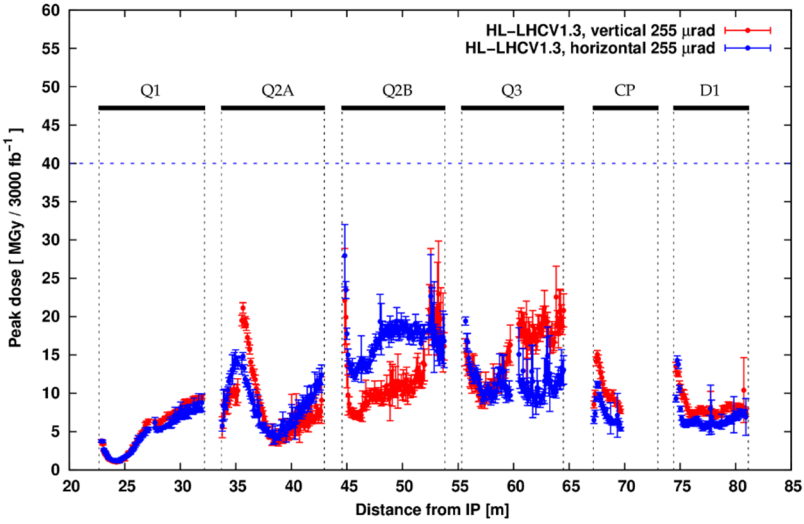

Fig. 2. Peak dose profile in the superconducting coils of the single bore magnet string after 3000 fb^{-1}, for horizontal (blue) and vertical (red) crossing.

For the same instantaneous luminosity, the total power collected by the 60 m long string of magnets amounts in the worst case (vertical crossing) to more than 1200 W, almost equally shared between the beam screen structure and the cold masses.

3. Matching Section Protection

The transition from the single bore vacuum chamber hosting the two counter-rotating beams to the two separate beam chambers is embedded in the TAN (Target Absorber Neutral), another massive absorber, with a 3.3 m long copper core, aimed at intercepting the neutral component of the collision debris, mostly photons and neutrons. The TAN absorber provides a substantial protection to the double bore recombination dipole (D2) and the four main quadrupole assemblies of the matching section (see Figure 3, left panel), including dipole correctors. However, the HL-LHC layout features the D1–D2 distance shortening, implying a lower beam separation in the TAN, coupled to a very significant enlargement of its twin pipes, due to optics requirements. These design changes, together with an almost double-crossing angle and an important increase of the mechanical aperture of the upstream elements, bring a flagrant weakening of the TAN effectiveness, further aggravated by the luminosity rise. Therefore, the cold magnet shielding has to be strengthened, by complementing the TCL (Target Collimator Long) physics debris collimators on the outgoing beam with tungsten alloy warm masks put in front of the cryostats and matching the aperture of the following beam screen, without altering the magnet design. The incoming beam bore benefits from the presence of the TCT (Target Collimator Tertiary) collimators that, while cleaning by design the incoming halo, also play a role in intercepting the debris propagating in the opposite direction. This scheme prevents the risk of debris induced quenches, keeping the power density in the coils below 1 mW/cm^3 for the reference luminosity of 5×10^{34} cm^{-2} s^{-1}. Respective dose values after 3000 fb^{-1} are predicted to remain below 10 MGy, except for the D2, locally exceeding by 20% that threshold. In the less favorable case of horizontal crossing, where the leakage through the TAN is maximized, the total power collected by the D2, which is the most exposed magnet, amounts to 33 W, twice as much its load for vertical crossing.

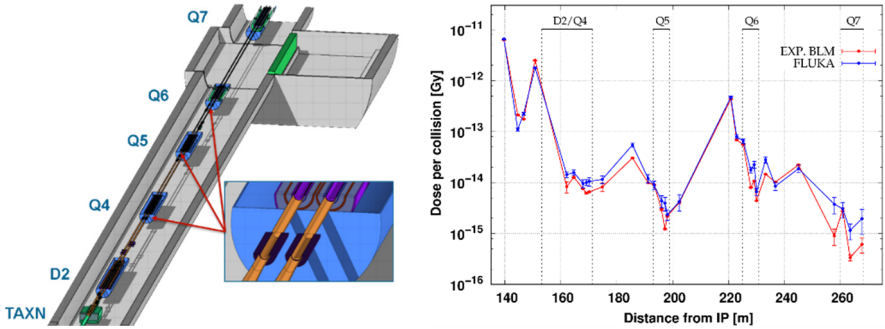

Fig. 3. Left: Geometry model of the future matching section layout. The frame zooms in on the additional TCLM masks. Right: BLM data (red) and FLUKA predictions (blue) in the present IR1 matching section for the fill #4919 of May 2016.

The matching section hot spots are displayed in the pattern of Beam Loss Monitor (BLM) data in the right panel of Figure 3, referring to the present machine layout. The first two points at about 140 m from the IP correspond to the front and rear of the TAN, while the following three peaks occur at the TCL locations, reflecting their different opening, with the TCL5 at about 185 m featuring a quite relaxed gap. The agreement quality in the absolute comparison with the simulation results gives a good confidence in the understanding of these medium distance losses, still critical even if representing only a few percent of the collision debris power.

4. Dispersion Suppressor Protection

The most forward TCL collimator, in the straight section half-cell 6, can provide a good cleaning of the initial part of the Dispersion Suppressor (DS) too, where the beam lines are bent by the LHC main dipoles, and no layout modification is planned for the HL-LHC era in IR1 and IR5. Nevertheless, beyond the TCL6 range, losses are expected in the DS odd half-cells, according to the periodicity of the single turn dispersion, and were already regularly observed, as shown by the BLM pattern in the left panel of Figure 4. In fact, they originate from protons subject to diffraction at the IP, affected by a magnetic rigidity deficit of the order of 1% and therefore destined to touch the horizontal boundary of the mechanical aperture towards the center of the ring.

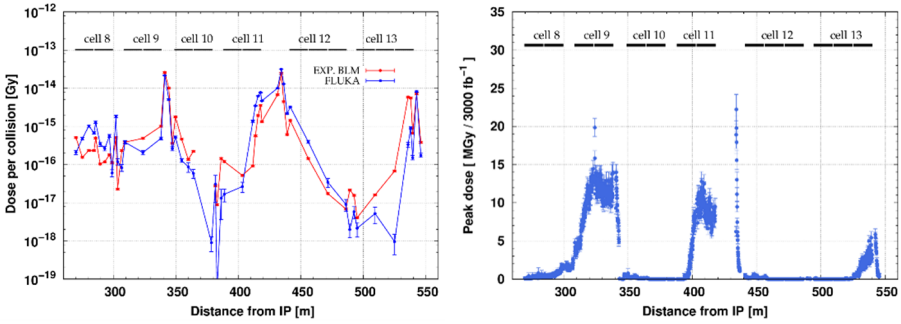

Fig. 4. Left: BLM data (red) and FLUKA predictions (blue) in the present IR5 DS for the fill #5401 of October 2016. Right: Peak dose profile in the superconducting coils of the DS magnets after 3000 fb^{-1} for horizontal crossing.

As a consequence, the right panel of Figure 4 presents the predicted peak dose profile in the superconducting coils for the accumulation of a 3000 fb^{-1} integrated luminosity, where the pronounced maximum at the end of the half-cell 11 is enhanced by an artificial aperture step in the simulation model at the specific interconnect between the missing dipole and the quadrupole assembly. On the other hand, actual imperfections in the machine aperture may locally worsen the picture, as well as more relaxed TCL6 gaps induce a dose increase up to the middle of the half-cell 9. In the latter, the main quadrupole cryostat hosts a dipole corrector, for which the resulting values, insensitive to the TCL6 setting, are deemed to be excessive on the left of IP1 and IP5 (taking into account the layout asymmetry), due to its lower radiation resistance, and mitigation actions, such as the introduction of an orbit bump, are being considered.

Respective peak power densities are of the order of 1 mW/cm^3 for the reference instantaneous luminosity of 5×10^{34} cm^{-2} s^{-1}.

5. Radiation to Electronics

Radiation damage to electronics is often considered for space applications. However, it is important to note that the radiation environment encountered at the LHC, the high number of electronic systems and components partly exposed to radiation, as well as the actual impact of radiation induced failures strongly differ from the context of space applications. While for the latter application design, test and monitoring standards are already well-defined,

additional constraints, but in some cases also simplifications, have to be considered for the accelerator environment.

The mixed particle type and energy field encountered in the relevant LHC areas is composed of charged and neutral hadrons (protons, pions, kaons and neutrons), photons, electrons and muons ranging from thermal energies up to the GeV range. This complex field has been extensively simulated by the FLUKA Monte Carlo code and benchmarked in detail for radiation damage issues at the LHC. The observed radiation is due to particles generated by proton-proton (or ion-ion) collisions in the LHC experimental areas (as previously discussed in this chapter), beam losses (protons, ions) on the collimators, and distributed interactions of the beam with the residual gas inside the beam pipe. The proportion of the different particle species in the field depends on the distance and on the angle with respect to the original loss point, as well as on the amount (if any) of installed shielding material. In this environment, electronic components and systems exposed to a mixed radiation field will experience three different types of radiation damages: these are displacement damage, damage from the Total Ionising Dose (TID) and so-called Single-Event-Effects (SEEs). The latter range from single or multiple bit upsets (SEUs or MBUs), transients (SETs) up to possible destructive latch-ups (SELs), destructive gate ruptures or burn-outs (SEGRs and SEBs).

The first two groups are of cumulative nature and are measured through TID and non-ionizing energy deposition (NIEL, generally quantified through accumulated 1-MeV neutron equivalent fluence), where the steady accumulation of defects cause measurable effects which can ultimately lead to device failure. As for stochastic SEE failures, they form an entirely different group as they are due to the localized ionization by a single particle, able to deposit sufficient energy through ionization processes in order to perturb the operation of the device. They can only be characterized in terms of their probability of occurring as a function of accumulated High Energy (>20 MeV) Hadron (HEH) fluence. The probability of failure will strongly depend on the device as well as on the flux and nature of the particles. In the context of HL-LHC, several tunnel areas close to the LHC tunnel, and partly not sufficiently shielded, are or are supposed to be equipped with commercial or not specifically designed electronics, which are mostly affected by the risk of SEEs [10], whereas electronics installed in the LHC tunnel will also suffer from accumulated damage in the long-term.

The impact of radiation effects on the accelerator performance and availability can be in first term quantified by the number of beam dumps induced by SEE failures in critical equipment. In addition to the premature loss of the beam and as opposed to non-destructive SEEs, typically solved by a remote reset, destructive SEEs will also require an access to the machine for replacement, and therefore will induce machine downtime.

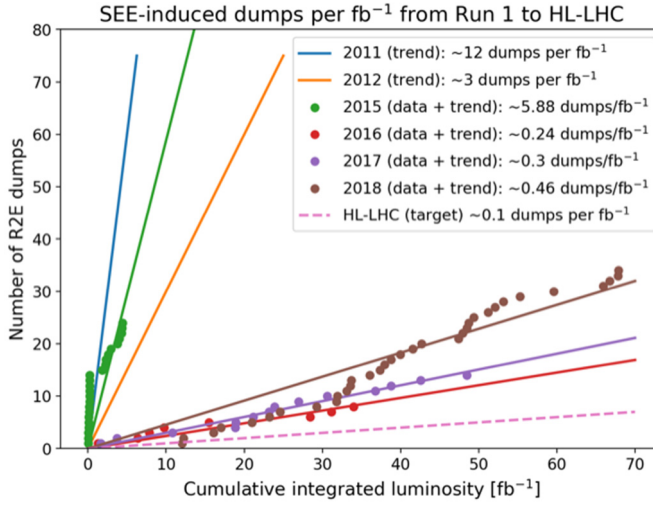

Fig. 5. Number of SEE induced dumps as a function of integrated luminosity for Run 1 and Run 2, and HL-LHC requirement.

Therefore, the number of SEE dumps per unit integrated luminosity can be used as a figure-of-merit of the R2E impact on the machine availability and is shown in Figure 5 with Run 1 and Run 2 data and HL-LHC objectives. Thanks to the LS1 mitigation measures and the Run 2 deployment of radiation tolerant systems, the <0.5 dump/fb^{-1} requirement was fulfilled. Further development and qualification activities within the R2E project are aimed at meeting the challenging <0.1 dump/fb^{-1} requirement for HL-LHC operation.

In addition to SEE effects, which scale linearly with integrated radiation levels and start manifesting from a very early stage in the accelerator operation, cumulative radiation damage is also a threat for the availability of critical accelerator systems, and will not manifest itself through a linear behavior with the accumulated radiation levels, but rather as a prompt failure increase, as

described in the wear-out phase of the so-called reliability bathtub curve. Therefore, the design and qualification of systems compliant with the radiation lifetime requirements is an essential ingredient to the Radiation Hardness Assurance procedure, in addition to the SEE tolerance.

Hence, defining the radiation levels to which a certain HL-LHC system will be exposed to is an essential step to be completed at a very early stage of the design specification [11]. The expected radiation levels will have an impact on the high-level system architecture as well as on the selection of electronic components and their qualification strategy.

A broad variety of radiation environments and levels are encountered in a high-energy hadron accelerator like the LHC, with gradients that can involve order of magnitude changes over just a few meters distance. As a general guideline, the radiation level intervals and respective recommendations for electronic component use are summarized in Table 1.

Table 1. Radiation level intervals and respective recommendations for electronic component use.

Lifetime Dose (Gy)	Lifetime n_{eq} fluence (cm^{-2})	Annual HEH fluence (cm^{-2} yr^{-1})	R2E Category
<10	$<10^{11}$	10^{6}-10^{9}	Only SEEs are of concern
10-200	10^{11}-2×10^{12}	10^{9}-2×10^{10}	Standard qualification for LHC tunnel equipment; both SEEs and cumulative damage are of concern
200-3000	2×10^{12}-3×10^{13}	2×10^{10}-3×10^{11}	Dose interval in which most standard COTS will fail; component level SEE qualification might require Heavy Ions; system level tests in CHARM will require multiple weeks
>3000	$>3\times10^{13}$	$>3\times10^{11}$	Use of COTS typically excluded

In the rest of this chapter, we will cover several examples of radiation levels in the vicinity of IP1 and IP5 for the HL-LHC operation, where, as previously discussed, the source of the radiation environment is the collision debris.

5.1. *Triplet and Matching Section*

The respective dose levels as calculated with FLUKA at beam height and 1.6 m distance from the beam line towards the inside of the ring can be seen

in Figure 6. They remain above 10 kGy up to a 230 m distance from the IP. Therefore, this region is essentially excluded for commercial-off-the-shelf (COTS) components, and related accelerator equipment needs to be hosted in shielded areas, such as the UJs, ULs and RRs, which will be covered later.

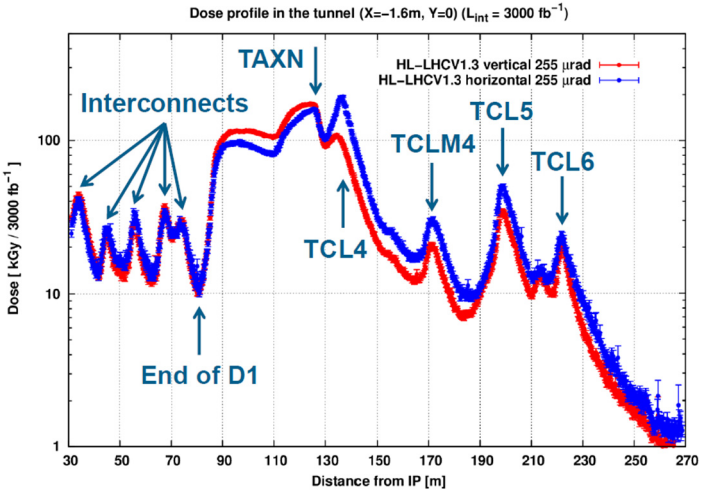

Fig. 6. Dose profile at beam height and 1.6 m from the machine axis on the internal side of the HL-LHC straight section, for vertical (red) and horizontal (blue) crossing.

Of particular interest in this interval is the area near the end of D1, which is a possible location for the cold by-pass diodes of the triplet to potentially suffer from radiation damage. The calculated radiation levels around this area can be seen in Figure 7, referring to different heights (60, 80 and 100 cm) above the vacuum chamber. Just downstream the D1, at about 83 m from the IP, where the cold-diode would be located[†], one finds at a height of 80 cm roughly 30 kGy and 1.5×10^{14} n_{eq}/cm^2 for the nominal HL-LHC lifetime, which can therefore be considered as specification values, excluding safety margins, for the respective diode radiation qualification.

[†] Detailed integration studies for the cold diode location are presently ongoing, in addition to further FLUKA simulations taking into consideration a more detailed description of the surroundings of the diode (e.g. diode box, DFX connection, etc.).

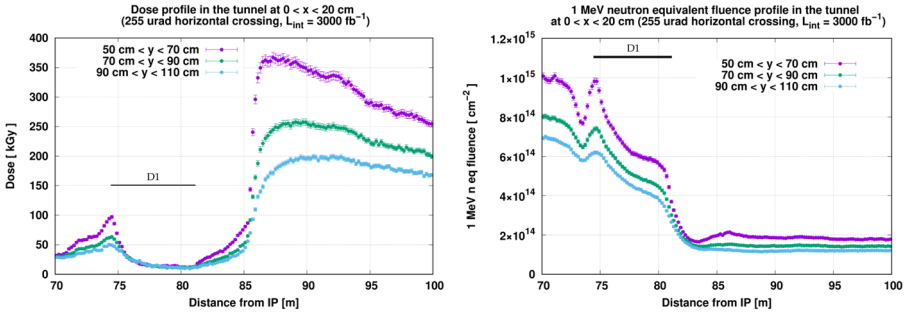

Fig. 7. Dose and 1-MeV neutron equivalent fluence in the area of the triplet-D1 string cold diode.

It is interesting to note that the D1 magnet on the one hand acts as shielding for the dose, which increases abruptly after its end, and as a neutron source on the other hand, as indicated by the following lower fluence plateau. As a consequence, finding an optimal position both in terms of ionizing dose and 1-MeV neutron equivalent becomes challenging. However, it is worth noting that in the specific case of the cold diodes, the main degradation mechanism is linked to an increase in the forward voltage related to displacement damage, therefore the neutron equivalent fluence is the main requirement from a radiation standpoint.

5.2. *Dispersion Suppressor*

As presented in Section 4, the Dispersion Suppressors of the high luminosity insertions feature pronounced losses in the odd half-cells. Focusing here on the equipment below the cryostats, Figure 8 shows the calculated dose profile, highlighting the regions that exceed the standard LHC tunnel qualification target of 200 Gy. As a consequence, extended intervals of the HL-LHC DS will either be excluded for equipment qualified up to 200 Gy, or host equipment (i) requiring periodic planned replacement and/or (ii) tolerant up to larger levels.

It is to be noted that, whereas relocation is a valid solution to spare the equipment from the very large radiation levels of the areas where their associated objects are operated (for instance, power converters and Quench Protection System versus their corresponding magnets), it often comes at a

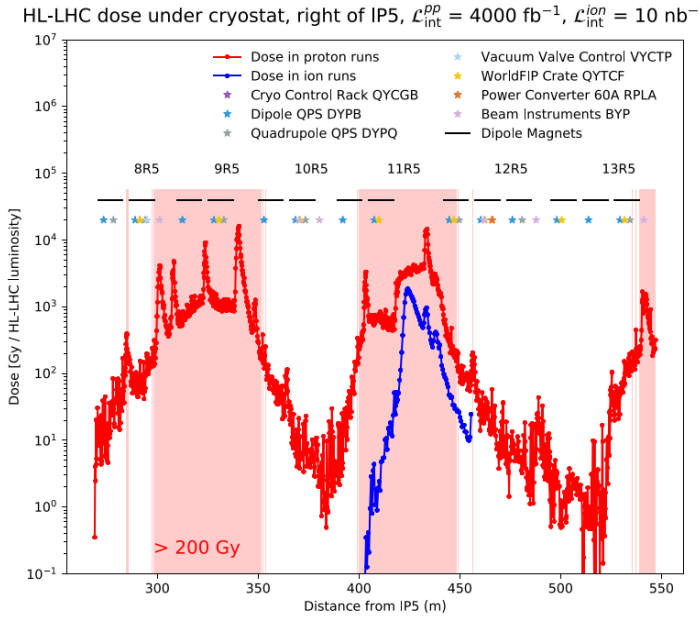

Fig. 8. HL-LHC radiation levels in the IR5 Dispersion Suppressor. A similar profile is expected for IR1.

high cabling cost, and therefore needs to be adequately balanced out with respect to the achievable radiation tolerance of the system.

Moreover, electronics in the DS will also be subject to very large particle fluence, which can have an impact in terms of possible displacement damage degradation, as well as, notably, SEEs.

5.3. *Shielded Areas*

In order to host electronic systems for equipment in high radiation areas, shielded alcoves were included in the LHC infrastructure. For IR1 and IR5, the most relevant alcoves, from the point of view of their still challenging radiation levels, are the UJs (Junction Chamber), ULs (Liaison Gallery between underground works) and RRs. As can be seen in Figures 9 and 10, the expected high energy hadron fluence for one HL-LHC year in these areas is as large as 10^{10} HEH/cm^2, corresponding to roughly 10 Gy/yr and 10^{11} n_{eq}/cm^2.

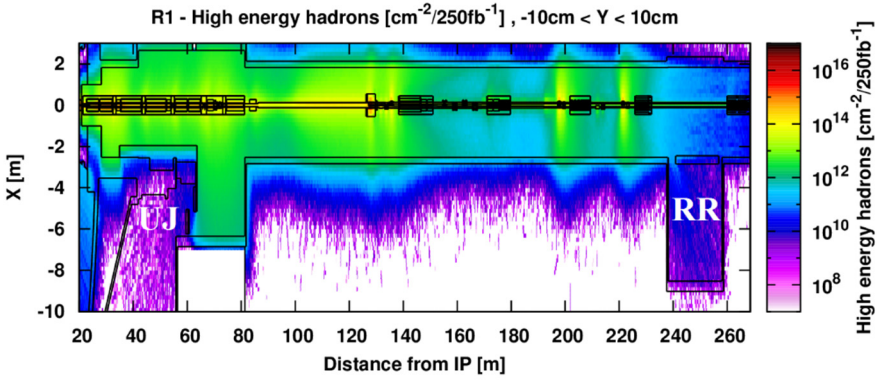

Fig. 9. HL-LHC annual high-energy hadron fluence in the IR1 straight section, including the RR and UJ shielded areas.

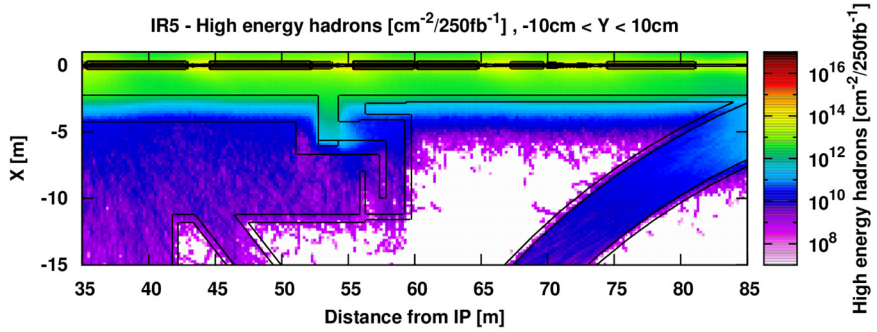

Fig. 10. HL-LHC annual high-energy hadron fluence in the IR5 triplet-D1 region, including the UJ shielded area.

In addition to Single Event Effects, which are presently the only concern for the LHC shielded areas, these levels will also potentially induce cumulative degradation of the electronics and therefore will also represent a threat to its lifetime.

5.4. *Implications on Radiation Hardness Assurance*

The radiation levels introduced above, along with the performance and availability requirements for the HL-LHC and its systems (for instance, many of the distributed systems exposed to radiation can only afford one

single radiation induced failure leading to a beam dump per year), imply a highly challenging Radiation Hardness Assurance approach for the HL-LHC equipment.

The associated methodology combines critical component level testing up to the typical requirement, as well as system level testing in the highly representative radiation environment of the CHARM facility [12]. In CHARM, a mixed-radiation field for the qualification of accelerator equipment is generated through the interaction of a 24 GeV/c proton beam with a 50 cm copper target.

In fact, the availability of a facility such as CHARM, unique in the world as for its capability of irradiating full large-scale systems with a radiation environment representative of the one present in the LHC accelerator, is the cornerstone of the associated qualification approach.

System level radiation tests in CHARM are typically performed on a weekly basis, corresponding to roughly 10^{16} protons on target, and during which the equipment receives a dose (depending on the actual irradiation configuration) of roughly 200 Gy, therefore compliant with the typical tunnel and shielded area radiation level requirements. As an example, the FGClite power converter controls and the 600A and 4-6-8 kA converters have been already tested in CHARM according to the HL-LHC radiation level and availability requirements.

References

1. T. T. Bohlen, F. Cerutti, M. P. W. Chin, A. Fassò, A. Ferrari, P. G. Ortega, A. Mairani, P. R. Sala, G. Smirnov, and V. Vlachoudis, The FLUKA Code: Developments and Challenges for High Energy and Medical Applications, Nuclear Data Sheets 120, 211-214 (2014).
2. G. Battistoni et al., Overview of the FLUKA code, Annals of Nuclear Energy 82, 10-18 (2015).
3. S. Roesler, R. Engel, J. Ranft, The Monte Carlo Event Generator DPMJET-III, Proc. of the Monte Carlo 2000 Conference, Lisbon, A. Kling, F. Barao, M. Nakagawa, L. Tavora, P. Vaz eds., Springer-Verlag Berlin, 1033-1038 (2001).
4. A. Fedynitch, PhD Thesis, (2015). https://cds.cern.ch/record/2231593/files/, CERN-THESIS-2015-371.pdf.
5. L. S. Esposito et al., Power load from collision debris on the LHC Point 8 insertion magnets implied by the LHCb luminosity increase, IPAC2013, TUPFI022, p. 1382, (2013).

6. V. Vlachoudis, FLAIR: A Powerful But User Friendly Graphical Interface For FLUKA, Proc. Int. Conf. on Mathematics, Computational Methods & Reactor Physics, Saratoga Springs, New York, (2009).
7. A. Mereghetti et al., The FLUKA LineBuilder and Element DataBase: Tools for Building Complex Models of Accelerator Beam Lines, IPAC2012, WEPPD071, p. 2687, (2012).
8. N. V. Mokhov et al., "Protecting LHC IP1/IP5 Components Against Radiation Resulting from Colliding Beam Interactions," CERN-LHC-Project-Report-633, (2003).
9. N. V. Mokhov, I. L. Rakhno, "Mitigating radiation loads in Nb3Sn quadrupoles for the CERN Large Hadron Collider upgrades," Phys. Rev. STAB 9 (2006) 101001.
10. R. García Alía et al., "Single event effects in high-energy accelerators", Semicond. Sci. Technol., vol. 32, no. 3, p.034003 (Feb., 2017).
11. R. García Alía et al., "LHC and HL-LHC: Present and Future Radiation Environment in the High-Luminosity Collision Points and RHA Implications," in IEEE Transactions on Nuclear Science, vol. 65, no. 1, pp. 448-456 (Jan., 2018).
12. J. Mekki, M. Brugger, R. G. Alia, A. Thornton, N. C. D. S. Mota and S. Danzeca, "CHARM: A Mixed Field Facility at CERN for Radiation Tests in Ground, Atmospheric, Space and Accelerator Representative Environments," in IEEE Transactions on Nuclear Science, vol. 63, no. 4, pp. 2106-2114 (Aug., 2016).